Transport of Particulate Suspensions in Porous Media: Model Formulation

A mathematical model is formulated for the general class of problems that involve the transport of stable particulate suspensions in porous media. The porous medium is represented by a network of pore bodies (sites) and pore throats (bonds). Population balances for the species responsible for particle retention and permeability reduction are written in terms of the various mechanisms of particle capture and reentrainment. Rates of capture and release are evaluated using appropriate physical models. We specifically concentrate on mass transfer limited processes. The effective-medium theory is suitably formulated to determine the fluid flow distribution in the network and to calculate the permeability. The network representation of the porous medium together with the population balances and the rates of deposition and release provide a consistent model that finds application in filtration and fines migration processes.

M. M. Sharma
Department of Petroleum Engineering
University of Texas
Austin, TX 78712

Y. C. Yortsos
Departments of Chemical
and Petroleum Engineering
University of Southern California
Los Angeles, CA 90089

Introduction

The transport of particles as particulate suspensions in porous media is an important process with a variety of industrial applications ranging from filtration to fines migration in oil reservoirs. Due to its demonstrated industrial significance the subject has received considerable attention in the past. A large part of the early literature in filtration is associated with efforts to describe the performance of rapid sand filters used in water purification processes. A number of predictive models were developed essentially following the filtration equation proposed by Iwasaki (1937). An excellent description of such early work is presented in the review article by Herzig et al. (1970). A significant advancement in the theoretical understanding of the filtration process was recently achieved by the work of Payatakes et al. (1973) and Rajagopalan and Tien (1979), who imparted a new theoretical insight to the empirical correlations developed in the past.

A closely related class of problems of great practical importance involves the release of fine particles from pore bodies within the porous bed. The release of such fines from pore walls may be triggered by fluctuations in the pH of the injection fluid, the ionic strength, or the flow rate. Subsequently, the fines are convected along with the fluid until they are entrapped by pore throats at some point downstream (Sharma, 1985). Such a situation frequently arises in aquifers and oil reservoirs where pore lining clays adhering to the pore walls are released if a brine solution, which is incompatible to the formation, is brought into contact with the formation (Sharma et al., 1985). Since particle entrapment occurs primarily by size exclusion, rapid and dramatic reductions in permeability result. This damage is almost always irreversible and may require expensive cleanup operations such as acidizing. Khilar and Fogler (1983), provided a basic understanding of the process of fines release and subsequent entrapment.

In the present paper an attempt is made to consider the basic local mechanisms of particle release and capture and to quantitatively incorporate their effects into population balance equations. The permeability reduction is modeled using network models that provide a more accurate description of the process than permeability-porosity type correlations used in the past.

Model Formulation

The rates of deposition and release of particles within a porous medium are determined by the forces of interaction between the filter medium, the carrier fluid, and the suspended particles. Such interaction occurs due to (Tien and Payatakes, 1979; Rajagopalan and Kim, 1981; Dahneke, 1975)

a. Electrostatic forces
b. Hamaker or dispersion forces
c. Born repulsion
d. Hydrodynamic and gravitational forces
e. Mechanical stresses

An order-of-magnitude analysis of the various forces quickly demonstrates that under typical conditions some forces predom-

inate. For example, inertial effects are almost always negligible for the typically small Reynolds numbers in a porous medium (Herzig et al., 1970), whereas gravitational forces are of importance only for particles larger than 10 μm in size. The present analysis proceeds under the above assumptions. Therefore, the results obtained would be applicable to stable suspensions only (small settling velocities).

Following Larson (1978), the porous medium is represented as a network of sites and bonds with pore bodies identified as sites, and pore throats as bonds. Adjacent pore bodies are connected by pore throats, the number of pore throats emanating from a pore body being the coordination number Z of the porous medium. For typical consolidated porous media, Z ranges between 6 and 14. Pore throats are assumed to occupy negligible volume in comparison to pore bodies, which are taken to contribute most significantly to porosity. Permeability reduction is assumed to occur through the following two distinct mechanisms:

1. Particles larger in size than a given pore throat size are trapped by the pore throat, thus reducing the area allowed for fluid flow;
2. Particles of size significantly smaller than a given pore size deposit uniformly over pore bodies and pore throats, thus causing a gradual reduction of the pore throat radii

The two postulated mechanisms represent the limiting cases of fines migration and filtration processes, respectively. In either case, complete reduction of permeability (plugging) occurs when a sufficient number of pore throats are blocked to reduce the conductivity of the medium to zero.

Following Khilar and Fogler (1983) the species of interest in the present model are:

1. The suspended particles (s)
2. The attached particles (A)
3. The trapped particles (T)
4. The unblocked pore throats (p)

Each particle species (i) is characterized by a local volumetric concentration ρ_i and size distribution f_i, while the unblocked pore throats are characterized by a volumetric concentration N_p and a size distribution f_p. This is shown schematically in Figure 1 (Khilar and Fogler, 1983). The pore throat and particle size distributions play a critical role in determining the rates of particle trapping. Furthermore, the permeability of the porous medium is computed based on the size distribution of open pore throats.

Assuming negligible dispersion, a general population balance for the suspended particles is of the form

$$q\frac{\partial \rho_s f_s}{\partial x} + \phi\frac{\partial \rho_s f_s}{\partial t} = \text{(Rate of release or deposition due to surface forces) + (Rate of mechanical trapping at pore throats) + (Rate of generation or disappearance due to coagulation)} \quad (1)$$

Similarly, one obtains for the unblocked pore throats,

$$\frac{\partial N_p f_p}{\partial t} = \text{(Rate of generation or disappearance due to pore size reduction by smooth deposition) − (Rate of blocking due to mechanical trapping at pore throats)} \quad (2)$$

In the above, the particle and pore concentrations ρ_s and N_p are expressed as number per pore volume and total volume, respectively, while q is the superficial flow velocity. Similar equations can be written for the attached and trapped particles. The terms on the righthand side of Eqs. 1 and 2 include deposition, release, and trapping due to distinctly different mechanisms. These rates are expressed per unit total volume and are evaluated quantitatively in the following sections.

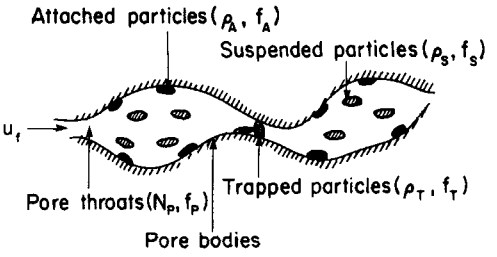

Figure 1. Physical system and species of interest.

Rates of deposition and release of particles

For Brownian particles, when diffusion and surface interactions dominate, the description of the process near a pore wall is furnished by Smoluchowski's equation. In the presence of a significant energy barrier ($E^{act} > 10\,KT$) and following a pseudosteady-state approximation, Ruckenstein and Prieve (1976) obtained the following expressions for the rates of particle release or deposition

$$k'_{rel} = D(H_{max})\left(\frac{\upsilon_{max}\upsilon_{min}}{2\pi KT}\right)^{1/2}\exp\left(-\frac{V_{Tmax} - V_{Tmin}}{KT}\right) \quad (3)$$

$$k''_{dep} = D(H_{max})\left(\frac{\upsilon_{max}}{2\pi KT}\right)^{1/2}\exp\left(-\frac{V_{Tmax}}{KT}\right) \quad (4)$$

υ_{max} and υ_{min} denote $\partial^2 V_T/\partial H^2$ evaluated at H_{max} and H_{min}, respectively. Note that k'_{rel} has dimensions of $(\text{time})^{-1}$, while k''_{dep} has dimensions of $(\text{length})(\text{time})^{-1}$.

A typical plot of the potential energy diagram is shown in Figure 2. Included in the calculations are hydrodynamic retardation effects (Sharma, 1985), while the expressions used for Hamaker and electrostatic interactions and Born repulsion are listed in the supplementary material. Also shown in Figure 2 are the activation energies for deposition and release E^{act}_{dep}, E^{act}_{rel}.

In the absence of an appreciable energy barrier, or when the potential energy is completely attractive or repulsive, the dominant resistance to particle transfer lies in the diffusion boundary layer. Since the process is now limited by external mass transfer, the pseudosteady-state assumption made above is no longer valid. The surface acts as a perfect source or sink, and the surface boundary condition must be suitably modified. The transition from kinetic to mass transfer control for particle deposition over spherical collectors was investigated by Jang (1983). Proceeding in an analogous fashion we postulate that, in this case, the particle flux to the capillary surface is provided by the perfect source or sink solution derived by Levich (1962) for Poiseuille flow,

$$j' = 0.67\rho_s D\left(\frac{2u_R}{Dr_p z_p}\right)^{1/3} \quad (5)$$

where u_R is the mean fluid velocity in a pore of radius r_p, and z_p is the distance along the pore.

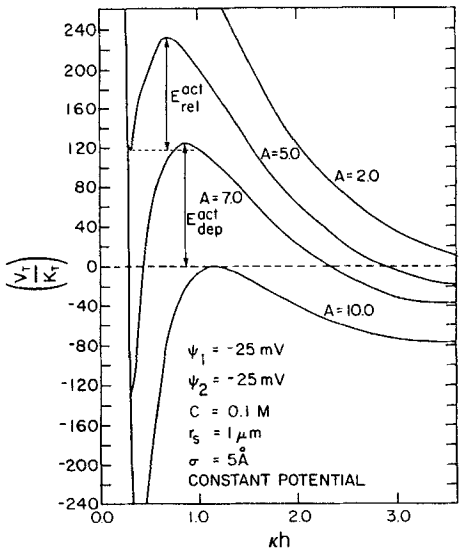

Figure 2. Typical potential energy diagram for deposition and release.

Completely repulsive case, $A = 2.0 \times 10^{-14}$ erg.
Completely attractive case, $A = 10 \times 10^{-14}$ erg.

We can integrate Eq. 5 over the pore surface area to obtain a kinetic constant for deposition (Sharma, 1985)

$$k'_{dep} = 2D(2u_R l_p^2/Dr_p)^{1/3}/r_p l_p \qquad (6)$$

For deposition at kinetic control we use Eq. 4 and follow an identical procedure to obtain

$$k'_{dep} = k''_{dep} 2/r_p \qquad (7)$$

In the case of particle release, the kinetic constant is given by Eq. 6 for external mass transfer control, and by Eq. 3 for kinetic

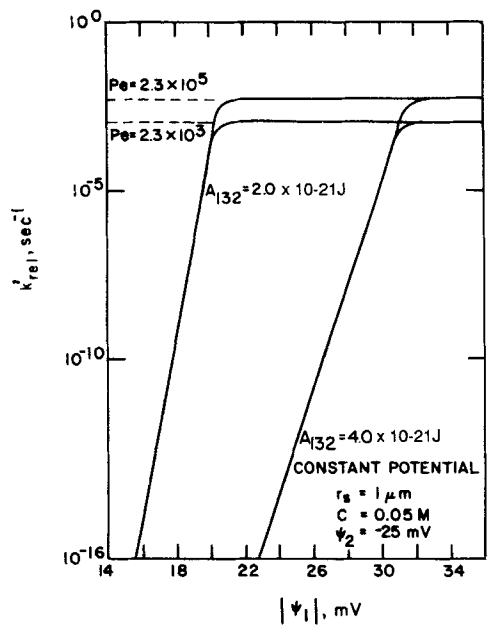

Figure 3. Rate of release as a function of surface potential ψ_1.

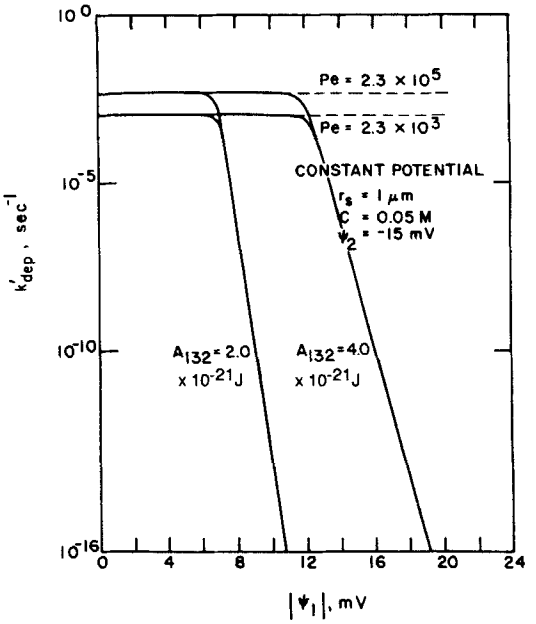

Figure 4. Rate of deposition as a function of surface potential ψ_1.

control. The results obtained for particle release are shown in Figure 3. In this illustration (Hamaker constant $A_{123} = 2 \cdot 10^{-14}$ erg) as the surface potential ψ_1 is increased from 16 to 21 mV, the rate constant of release increases from 10^{-16} s^{-1} to an upper limit specified by the perfect-source solution. This upper bound is a function of the local Peclet number and increases with increasing flow rates and decreasing pore sizes. A similar behavior is observed with the rate of deposition, which increases very rapidly to its maximum value as the surface potential is lowered, Figure 4. Figures 3 and 4 are based on the constant potential interaction assumption. Qualitatively similar results are also obtained for constant charge or mixed boundary conditions (Sharma, 1985; Sharma et al., 1985).

Based on the above results it is possible to construct curves such as those shown in Figure 5. Here, regions in the $(\psi_1 - \psi_2)$

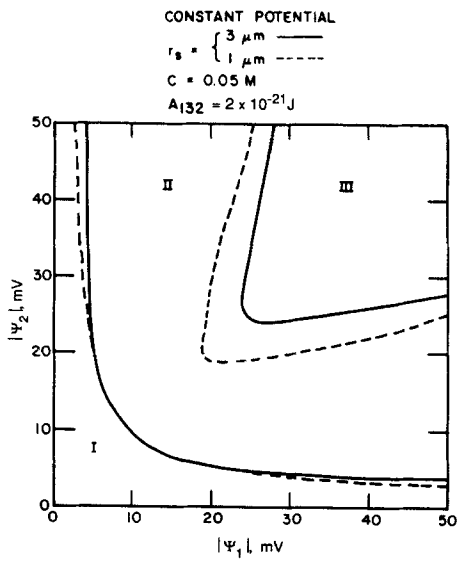

Figure 5. Effect of particle radius r_s on stability diagram.

plane are delineated where deposition or release is the dominant mechanism for typical flow conditions. In region I the rate of deposition is given by the perfect-sink solution, in region II neither deposition nor release rates are significant, and in region III the release rate is given by the perfect-source solution. It follows that most situations of practical interest in filtration or fines migration processes would fall in region I or III, with rates determined by the perfect-sink or the perfect-source solution, respectively.

The above analysis was based on Brownian particles. Similar conclusions can also be drawn from the results of the work by Payatakes et al. (1974a,b) for non-Brownian particles. Rate calculations using trajectory analysis have shown that the rate of deposition decreases sharply at a critical value of the London, van der Waals, and electrostatic surface force parameters. It is possible therefore to construct stability diagrams similar to Figure 5 using a trajectory analysis. However, it not clear at present how the trajectory analysis can be applied to estimate rates of particle removal from surfaces.

To estimate the macroscopic rates of deposition or release, we make use of the perfect-source/sink solution. For a porous medium with a pore size distribution f_p and a pore density per total volume N_p, the overall rate expressed in number of particles per total volume and time is the integral over all pore sizes of the particle flux for a single pore j

$$J_{rel/dep} = N_p \int_0^\infty j f_p(r)\, dr = k_{rel/dep}\rho_s \tag{8}$$

Then, it can be directly shown that

$$k_{rel/dep} = 2\pi D^{2/3} l_p^{2/3} N_p \int_0^\infty (2r^2 u_R)^{1/3} f_p\, dr \tag{9}$$

Network flow distribution

The preceding analysis shows that for Brownian particles, surface interactions determine whether deposition or release will occur. However, the corresponding rates are determined by the perfect-source or perfect-sink solution. The latter are implicit functions of the local flow velocities through individual pores. To obtain an exact solution to the problem of the network flow distribution, a Monte Carlo numerical simulation would have to be used. As an alternative, the flow velocity distribution may be estimated using the effective-medium theory (EMT) (Kirkpatrick, 1973; Koplik, 1982). The derivation shown in the Appendix provides an expression for the mean fluid velocity u_R in pores of radius r_p

$$u_R = \frac{q r_p^2}{8k}\left[1 + \frac{r_m^4 - r_p^4}{r_p^4 + \left(\frac{Z}{2} - 1\right) r_m^4}\right] \tag{10}$$

This result shows the significant effect of the coordination number Z on the flow velocity distribution. At $Z \to \infty$ the expression for the capillary tubes model is recovered. Equations 9 and 10 provide a convenient formalism for expressing the rates of deposition and release.

Pore closure due to deposition on pore walls

When the diameter of the particles is much smaller than the diameter of the pore throats no trapping will occur, due to size exclusion. However, permeability reduction is still observed in such cases, even though it is a much slower process. This reduction is caused by the deposition of particles on the pore walls. This is the dominant mechanism of particle attachment when an attractive surface potential energy exists between the filter medium and the fines. For the case of mass transfer control discussed in this paper, the rate of pore closure is given by

$$\frac{dr_p}{dt} = -\rho_s V_s \left(\frac{2u_R D^2}{r_p l_p}\right)^{1/3} \tag{11}$$

where V_s is the mean volume of the deposited particles and l_p the mean pore length.

Trapping of particles due to size exclusion

To derive local rates for particle removal due to mechanical entrapment, we focus our attention on a representative volume of the porous medium with a statistically large number of pores. As in the previous analysis, we assume that fluid flows through the medium at a constant superficial velocity q. We next denote by n the average number of pore throats a fluid particle encounters in the volume element before emerging from it. If Δt is the time taken for the fluid to traverse the volume element (Bodziony and Litwiniszyn, 1962) then

$$n = \frac{q\Delta t}{\phi l_p} \tag{12}$$

where the pore length l_p is assumed constant. As the fluid carries suspended particles, a certain fraction of the latter is trapped by the pore throats at each of the n steps. If the fraction of particles of size in the interval $(r_s < r < r_s + dr_s)$ trapped at each step is $P(r_s)$, the mass balance on particles of this size at the conclusion of the ith step reads as follows,

$$(\rho_s f_s)_i = (\rho_s f_s)_{i-1}[1 - P(r_s)] \tag{13}$$

$$P(r_s) = \frac{\text{no. of particles in } (r_s, r_s + dr_s) \text{ trapped in } i\text{th step}}{\text{no. of particles in } (r_s, r_s + dr_s) \text{ before } i\text{th step}} \tag{14}$$

We proceed by assuming that the above probability of trapping is constant at each particle step. At the end of n steps the fraction of particles trapped by the sequence of n steps, P_t, assumed independent, is given by

$$P_t = P(r_s)\sum_{i=1}^{n}[1 - P(r_s)]^{i-1} = 1 - [1 - P(r_s)]^n \tag{15}$$

The number per unit pore volume of particles in the size interval $(r_s, r_s + dr_s)$ that are trapped by pore throats in the time interval Δt is therefore equal to

$$\frac{\rho_s f_s}{\Delta t} P_t dr_s = \frac{\rho_s f_s q dr_s}{\phi l_p}\left\{\frac{1 - [1 - P(r_s)]^n}{n}\right\} \tag{16}$$

The case when p is of order one is trivial, as it implies instantaneous particle trapping. For the most interesting case $P \ll 1.0$,

we have $(1 - P)^n \cong 1 - nP$, and the above expression reduces to

$$\frac{\rho_s f_s q}{\phi l_p} P(r_s) dr_s \tag{17}$$

If it is further assumed that the particles distribute themselves in the pores in the same proportion as in the fluid, then the fraction of particles approaching unblocked pore throats in the size interval $(r_p, r_p + dr_p)$ is proportional to the corresponding flow rate partition,

$$\frac{N_p f_p r_p^2 u_R dr_p}{\int_0^\infty N_p f_p r_p^2 u_R \, dr_p} = \frac{I'(r_p)\, dr_p}{I(\infty)} \tag{18}$$

where we have denoted $I(r) = \int_0^r f_p r_p^2 u_R \, dr$. In the above, u_R is the fluid velocity through the pore throat shown in Eq. 10 estimated via the EMT; see the Appendix.

We thus obtain the rate of plugging of pores in the size interval $(r_p, r_p + dr_p)$ by particles of size in the interval $(r_s, r_s + dr_s)$

$$\frac{\rho_s f_s q P(r_s) dr_s}{\phi l_p} \cdot \frac{I'(r_p)}{I(r_s)} dr_p \tag{19}$$

However, pores of this size are effectively plugged by all particles of size greater than r_p. Thus the overall rate of pore closure for pores in the size interval $(r_p, r_p + dr_p)$ is

$$\frac{\rho_s q}{\phi l_p} \int_{r_p}^\infty \frac{f_s P(r_s) dr_s}{I(r_s)} I'(r_p)\, dr_p \tag{20}$$

Note that in the above discussion the assumption has been made that a particle, once trapped, blocks one pore throat completely. This assumption can in principle be relaxed, but the resulting analysis contains two additional structural parameters for the porous medium, which must be empirically determined. Such an analysis is discussed by Sharma (1985). For the present paper, a one-to-one correspondence is assumed to be adequate.

The preceding expressions involve the fraction $P(r_s)$ of particles that are retained at each step. To estimate $P(r_s)$ we proceed by postulating that the fraction of particles approaching an unblocked pore throat is proportional to the fluid flow rate through it. The fraction of particles that approach a pore in the interval $(r_p, r_p + dr_p)$ and are trapped by it is equal to

$$[1 - F_s(r_p)] \frac{I'(r_p) dr_p}{I(\infty)} \tag{21}$$

where

$$F_s = \int_0^{r_p} f_s \, dr \tag{22}$$

All trapped particles have sizes in the interval (r_p, ∞). Thus, the fraction of trapped particles that have size in the interval $(r_s, r_s + dr_s)$ is given by

$$\frac{I'(r_p) dr_p}{I(\infty)} f_s dr_s \tag{23}$$

Particles of size $(r_s, r_s + dr_s)$ will be trapped only by pore throats of size less than or equal to r_s. Therefore, the fraction of particles of size $(r_s, r_s + dr_s)$ trapped by pore throats smaller than r_s is obtained by integrating over all such pore throats

$$f_s \frac{I(r_s)}{I(\infty)} dr_s \tag{24}$$

Finally, using the definition of $P(r_s)$ in Eqs. 13 and 24 the fraction of particles of size $(r_s, r_s + dr_s)$ that are trapped at each step is

$$P(r_s) = \frac{I(r_s)}{I(\infty)} \tag{25}$$

All the above expressions are derived for fractions of particles based on the total number of particles present in the ith step, ρ_s. The corresponding numbers of particles per unit pore volume are obtained by simply multiplying by ρ_s.

Population balance equations

Population balance equations for the four species of interest—i.e., the attached particles ρ_A, f_A; the suspended particles ρ_s, f_s; the trapped particles ρ_T, f_T; and the pore throats N_p, f_p—can be written in terms of the rate equations discussed earlier. The overall population balances for ρ_A, ρ_s, ρ_T, and N_p can be obtained by integrating each of these equations over all radii.

It should be noted that the effect of the removal of non-Brownian particles by fluid shear forces is not included in the equations. In certain cases where high flow rates of carrier fluid are achieved, a number of particles may be entrained by the fluid due solely to hydrodynamic effects. Such terms can, in principle, be incorporated into the equations (Sharma, 1985). Similarly, additional important effects, such as coagulation of suspended particles, can also be incorporated but only serve to complicate the equations beyond the computational methods of solution developed in this work. Thus, at least as a first approximation, subsequent papers on this work (Sharma and Yortsos, 1987a,b) do not consider the effects of coagulation within the porous medium.

The dimensionless population balance equations may now be written as

$$\frac{\partial \rho_{AD} f_{AD}}{\partial t_D} = -(1 - \theta) ER \rho_{AD} f_{AD} + \theta ER \rho_{sD} f_{sD} \tag{26}$$

$$\frac{\partial \rho_{sD} f_{sD}}{\partial t_D} + \frac{\partial \rho_{sD} f_{sD}}{\partial x_D} = (1 - \theta) ER \rho_{AD} f_{AD} - \theta ER \rho_{sD} f_{sD} - \frac{I_D(r_{sD}/A)}{\mu I_D(\infty)} \rho_{sD} f_{sD} \tag{27}$$

$$\frac{\partial N_{pD} f_{pD}}{\partial t_D} = -\frac{B}{\mu} \frac{I'_D(r_{pD})}{I_D(\infty)} \rho_{sD} [1 - F_{sD}(r_{pD} A)] + \theta C N_{pD} \rho_{sD} \frac{\partial}{\partial r_{pD}} \left(f_{pD} \frac{u_{RD}^{1/3}}{r_{pD}^{1/3}} \right) \tag{28}$$

$$\frac{\partial \rho_{TD} f_{TD}}{\partial t_D} = \frac{I_D(r_{sD}/A)}{\mu I_D(\infty)} \rho_{sD} F_{sD} \tag{29}$$

In the above, particle concentrations are made dimensionless with respect to a characteristic concentration ρ_s^*, pore density with respect to the original pore density N_p^*, distance with respect to a macroscopic length L, and time with respect to the convective time $\phi L/q$, while particle and pore radii are made dimensionless with respect to the average sizes r_s^* and r_p^*, respectively. The variable θ takes the values 0 and 1 for the cases of particle release and deposition, respectively. The dimensionless groups emerging from the equations are:

$\mu = l_p/L$
$A = r_p^*/r_s^*$
$B = \phi\rho_s^*/N_p^*$
$C = \phi\rho_s^* LV_s(2D^2/l_p q^2 k_o r_p^{*2})^{1/3}$
$E = 2\pi N_p^* L(2D^2 l_p^2 r_p^{*4}/q^2 k_o)^{1/3}$

In addition, the following functional relations are used

$$u_{RD} = \frac{r_{pD}^2}{8k_D}\left[1 + \frac{r_{mD}^4 - r_{pD}^4}{r_{pD}^4 + (Z/2 - l)r_{mD}^4}\right] \tag{30}$$

$$R = N_{pD}\int_0^\infty (u_{RD} r_{pD}^2)^{1/3} f_{pD}\, dr_{pD} \tag{31}$$

$$I_D = \int_0^{r_D} u_{RD} r_{pD}^2 f_{pD}\, dr_{pD} \tag{32}$$

where k_D is a dimensionless permeability normalized with respect to its original value.

We briefly note that in the application of the equations to various processes, some of the terms become negligibly small. In particular, filtration processes are typically characterized by $\theta = 1$ (particle deposition), $A \gg 1$, while fines migration processes correspond to $\theta = 0$ (particle release), $A = 0$ (1). Related special cases are discussed in the companion papers.

Permeability reduction model

The dimensionless population balance equations provide concentration and size distribution profiles. However, a quantity of great interest, and one that is easily measurable experimentally, is the permeability of the porous medium.

A common approximation, often used in the past, involves the parallel capillary tubes model. The dimensionless permeability can then be expressed as,

$$k_D = \frac{\int_0^\infty r_p^4 N_p f_p(r_p, x, t)\, dr_p}{\int_0^\infty r_p^4 N_p f_p(r_p, x, 0)\, dr_p} \tag{33}$$

This model has some obvious shortcomings as it does not take into account the topology of the porous medium. Important parameters such as pore connectivity and accessibility are ignored. On the other hand, network models of finite coordination number have been shown to provide more accurate representations of porous media.

In a network model, the effective conductivity is a function of the bond conductivity distribution and the coordination number. In deriving the effective conductivity a conductance distribution $G(g_R)$ is assigned over the network. Although exact results have not been obtained, Kirkpatrick (1973) and Koplik (1981), have shown that for a broad class of conductance distributions, in a network sufficiently away from the percolation threshold, the effective medium conductivity g_m can be approximated from the solution of the integral equation

$$\int_0^\infty G(g_R) t(g_R)\, dg_R = 0 \tag{34}$$

where

$$t(g) = \frac{g_m - g_R}{g_R - \left(1 - \frac{Z}{2}\right)g_m} \tag{35}$$

Individual conductances are related to pore size via the expression

$$g_R \propto r^n \qquad (2 < n < 4) \tag{36}$$

For our purposes, the quantity of interest is simply the ratio of the instantaneous permeability to the original permeability, k/k_o, given by

$$k_D = \frac{k}{k_o} = \frac{g_m}{g_{mo}} \tag{37}$$

where g_{mo} is the initial effective conductance of the medium.

The network conductance may also be obtained using concepts from percolation theory. Specifically, near the percolation threshold, where EMT results break down, percolation theory provides scaling laws for the medium conductance. In addition, analytical results are available, although for a restricted class of networks such as Bethe lattices (Stinchcombe, 1974; Larson, 1978).

Conclusions

When the particles being filtered have sizes much smaller than the pore throats, particle capture or entrainment occurs by surface deposition or release. Based on the potential energies of interaction, regions in the parameter space of the surface potentials are delineated where deposition or release will be dominant. The boundaries of these regions are sensitive to the particle radius and ionic strength. Smaller particles are more easily deposited onto or removed from the solid surface, while low ionic strength causes particle deposition or removal to be retarded, for the constant surface potential boundary condition. Whereas the onset of deposition or release is governed by the potential energy of interaction, in several cases the respective rates are controlled by mass transfer, thus by the network fluid velocity distribution. Based on the EMT, a network velocity distribution is derived and the macroscopic rates are estimated.

The population balance equations formulated here incorporate the various rates of deposition and release. Within the assumptions made in this paper they constitute a complete model for the process. Based on the relative sizes of the particles and pore throats and on experimentally available values of the surface potentials, the dominant mechanisms of particle capture can be identified by a simple order-of-magnitude analysis of the various terms in the population balances. In certain special cases useful analytical solutions can be obtained. Such solutions provide a useful insight into the problems discussed in detail in subsequent papers on this work (Sharma and Yortsos, 1987a,b).

Notation

A_{123} = Hamaker constant
A = parameter, r_p^*/r_s^*
B = parameter, N_s^*/N_p^*
C = parameter
C_D = drag coefficient
d_g = grain diameter, L
D = diffusion coefficient L^2/T
E = parameter
E^{act} = activation energy, $ML^2 \cdot T^{-2}$
f = size distribution, L^{-1}
F = integral, Eq. 38
g_R = pore conductance, L^3
g_m = effective network conductance, L^3
G = conductance distribution, L^{-3}
h = separation distance, H/r_s
H = separation distance between particle and flat plate, L
I = integral, Eq. 34
j = particle flux, no./pore $\cdot$ T
j' = local particle flux, no. $L^{-2} \cdot T^{-1}$
J = overall flux, no. $L^{-3} \cdot T^{-1}$
$k'_{dep/rel}$ = local rate constant for deposition or release, T^{-1}
$k_{dep/rel}$ = overall rate constant for deposition or release, T^{-1}
k = permeability, L^2
K = Boltzmann constant, $ML^2 \cdot T^{-2o}K^{-1}$
l = effective pore length, L
L = macroscopic dimension of porous medium, L
n = number of steps
N_p = number of pores per total volume no. L^{-3}
p = pressure, $ML^{-1} \cdot T^{-2}$
$P(r_s)$ = fraction of particles retained per step
q = fluid superficial velocity, $L \cdot T^{-1}$
Q = volumetric flow rate through a pore, $L^3 \cdot T^{-1}$
r = particle, pore radius, L
R = parameter
R_e = Reynolds number
t = time, T
T = temperature, K
u_R = mean fluid velocity in pores of radius r, $L \cdot T^{-1}$
V_s = particle volume, L^3
V_T = total potential energy of interaction, $ML^2 \cdot T^{-2}$
x = distance along the length of the porous medium, L
X = fraction of open pores
X_c = percolation threshold
y = volumetric fraction of particles, no. L^{-3}
z_p = distance along a single pore, L
Z = coordination number of network

Greek letters

ϵ = dielectric constant
η = viscosity, $ML^{-1} \cdot T^{-1}$
θ = parameter
λ = filtration coefficient, L^{-1}
μ = parameter
ν = kinematic viscosity, $L^2 \cdot T^{-1}$
ρ = concentration, no. L^{-3}
σ = collision diameter, L
ϕ = porosity
ψ = zeta potential, $ML^2 \cdot T^{-2}$
κ = Reciprocal Debye Hückel length, L^{-1}

Subscripts

A = attached particles
dep = deposition
f = flowing fluid
max = maximum
min = minimum
o = original condition
rel = release
p = open pores
s = suspended particles
T = trapped particles
1 = surface 1, particle of radius r_s
2 = surface 2, flat pore wall

Appendix

The effective medium theory has been developed in the context of linear electrical networks by Kirkpatrick (1973) and Koplik (1981) and illustrated for fluid flow in networks by Koplik (1982). Essential in the development of the theory is the notion that the applied potential difference across any conducting bond in the network is a superposition of a uniform external field and a local fluctuating yield, the space average of which over a sufficiently large volume is zero. All the bonds in the network can therefore be replaced by bonds of uniform conductance g_m, the value of which is calculated by requiring that the average of the local fluctuations be zero (Kirkpatrick, 1973).

For fluid flow in a network, the pressure drop across a given pore is obtained by the superposition of the mean field m and the local fluctuating field f:

$$\Delta p_R = \Delta p_m + \Delta p_f \tag{A1}$$

Following Kirkpatrick (1973) we obtain at the suggestion of M. A. Sahimi (private communication, 1984)

$$\Delta p_f = \frac{\Delta p_m (g_m - g_R)}{g_R + \left(\frac{Z}{2} - 1\right) g_m} \tag{A2}$$

where g_R is the conductance of a bond of radius r_p and g_m is the effective conductance of the network, satisfying the following equation,

$$\int_0^\infty G(g_R) \left[\frac{g_m - g_R}{g_R + \left(1 - \frac{Z}{2}\right) g_m} \right] dg_R = 0 \tag{A3}$$

where $G(g_R)$ is the conductance distribution of the network. Equation A2 is obtained by assuming Poiseuille flow through each pore. Denoting by Q_R the volumetric flow rate through a pore across which a pressure drop Δp_R exists, we have

$$Q_R = g_R \Delta P_R / \eta_f = u_R \pi r_p^2 \tag{A4}$$

where η_f denotes carrier fluid viscosity, u_R is the mean velocity, and a conductance g_R is assigned to each pore. As Eq. A4 is analogous to Ohm's law, the local fluctuating field Δp_f in Eq. A2 follows by a straightforward application of the effective-medium theory (Kirkpatrick, 1973). The effective conductance g_m evaluated from Eq. A3 can then be shown to satisfy the equation

$$g_m \Delta p_m = \eta_f \int_0^\infty G(g_R) Q_R \, dg_R \tag{A5}$$

In view of Eqs. A1, A2, and A3, the mean flow velocity is expressed by

$$u_R = \Delta p_m r_p^2 \left[1 + \frac{g_m - g_R}{g_R + (Z/2 - 1) g_m} \right] / 8 \eta l_p \tag{A6}$$

The macroscopic pressure drop Δp across a macroscopic length L is related to Δp_m through the expression

$$\Delta p/L = \Delta p_m/l_p \tag{A7}$$

At the macroscopic level, Darcy's law is in effect dictating

$$q = k\Delta p/\eta_f L \tag{A8}$$

where k denotes permeability. It follows that Eq. A6 can be rearranged to yield

$$u_R = \frac{qr_p^2}{8k}\left[1 + \frac{g_m - g_R}{g_R + (Z/2 - 1)g_m}\right] \tag{A9}$$

Equations A9 and A3 constitute the desired network flow distribution in the spirit of the Effective Medium approximation and provide a direct correlation between a pore of size r_p and the corresponding mean velocity u_R. The expression can be put in a more useful form by noting that $g_R \propto r_p^4$ for cylindrical shaped pores of constant length

$$u_R = \frac{qr_p^2}{8k}\left[1 + \frac{r_m^4 - r_p^4}{r_p^4 + \left(\frac{Z}{2} - 1\right)r_m^4}\right] \tag{A10}$$

As anticipated, the above expression reduces in the limit of high coordination numbers to the typical velocity distribution obtained for the capillary tube model. Use of the latter results in a monotonic increase of flow rates with capillary radius, the maximum flow velocity occurring in pores with the largest radii. Numerical experiments conducted on lattices by Simon and Kelsey (1971) show, however, that the maximum flow velocities are associated with pores of size near the mean radius. Such a maximum is indeed predicted by Eq. A10, and it occurs at the radius r_p^*,

$$r_p^* = r_m\left(\frac{Z}{2} - 1\right)^{1/4} \tag{A11}$$

while the local velocity vanishes as $r_p \to 0$ and $r_p \to \infty$. This is in qualitative agreement with the numerical predictions. Therefore, it is evident that use of a capillary tube model for a porous medium will certainly lead to errors in the flow distribution.

Literature Cited

Bodziony, J., and J. Litwiniszyn, "Mathematical Approach to the Phenomenon of Colmatage of an n-fractional Suspension of Particles," *Bull. de l' Academie Polonaise des Sciences*, **X**(1), 43 (1962).

Dahneke, B., "Kinetic Theory of the Escape of Particles from Surfaces," *J. Colloid Interf. Sci.*, **50**, 89 (1975).

Herzig, J. P., D. M. Leclerc, and P. LeGoff, "Flow of Suspensions through Porous Media—Application to Deep Bed Filtration," *Ind. Eng. Chem.*, **62**, 8 (1970).

Iwasaki, T., "Some Notes on Sand Filtration," *J. Am. Water Works Ass.*, **29**, 1591 (1937).

Jang, L. K., "Modeling the Deposition of Bacteria in a Simple Hydrodynamic Field: Rate of Deposition onto a Spherical Collector," Ph.D. Diss., Univ. So. California (1983).

Khilar, K. C., and H. S. Fogler, "Water Sensitivity of Sandstones," *SPE J.*, **55** (1983).

Kirkpatrick, S., "Percolation and Conduction," *Rev. Mod. Phys.*, **45**(4), 574 (October 1973).

Koplik, J., "On the Effective Medium Theory of Random Linear Networks," *J. Phys. Chem.: Solid State Phys.*, **14**, 4821 (1981).

———, "Creeping Flow in Two-Dimensional Networks," *J. Fluid Mech.*, **119**, 219 (1982).

Larson, R. G., "Percolation in Porous Media with Application to Enhanced Oil Recovery," M. S. Thesis, Univ. Minnesota (1978).

Levich, V. G., *Physicochemical Hydrodynamics*, Prentice-Hall, Englewood Cliffs, NJ, 81–87 (1962).

Payatakes, A. C., C. Tien, and R. M. Turian, "A New Model for Granular Porous Media. I: Model Formulation," *AIChE J.*, **19**, 58 (1973).

———, "Trajectory Calculation of Particle Deposition in Deep Bed Filtration. I: Model Formulation," *AIChE J.*, **20**, 889, (1974a).

Payatakes, A. C., R. Rajagopalan, and C. Tien, "Application of Porous Media Models to the Study of Deep Bed Filtration," *Can. J. Chem. Eng.*, **52**, 727 (1974b).

Rajagopalan, R., and C. Tien, "The Theory of Deep Bed Filtration," *Progress in Filtration and Separation*, **1**, North Holland, New York, 179 (1979).

Rajagopalan, R., and J. S. Kim, "Adsorption of Brownian Particles in the Presence of Potential Barriers: Effect of Different Modes of Double-Layer Interaction," *J. Colloid Interf. Sci.*, **83**, 428 (1981).

Ruckenstein, E., and D. C. Prieve, "Adsorption and Desorption of Particles and Their Chromatographic Separation," *AIChE J.*, **22**, 276 (1976).

Sharma, M. M., "Transport of Particulate Suspensions in Porous Media: Applications to Filtration and Formation Damage in Sandstones," Ph.D. *Diss.*, Univ. So. California (1985).

Sharma, M. M., Y. C. Yortsos, and L. L. Handy, "Release and Deposition of Clays in Sandstones," Paper No. 13562, SPE Int. Symp. Oilfield Geothermal Chem., Phoenix (Apr., 1985).

Sharma, M. M., and Y. C. Yortsos, "A Network Model for Deep Bed Filtration Processes," *AIChE J.*, **33**(10), 1644 (Oct., 1987a).

———, "Fines Migration in Porous Media," *AIChE J.*, **33**(10), 1654 (Oct., 1987b).

Simon, R., and F. J. Kelsey, "The Use of Capillary Tube Networks in Reservoir Performance Studies. 1: Equal-Viscosity Miscible Displacement," *SPE J.*, **11**, 99 (1971).

Stinchcombe, R. B., "Conductivity and Spin-Wave Stiffness in Disordered Systems—An Exactly Soluble Model," *J. Phys. Chem.: Solid State Phys.*, **7**, 179 (1974).

Tien, C., and A. C. Payatakes, "Advances in Deep Bed Filtration," *AIChE J.*, **25**, 737 (1979).

Manuscript received Jan. 25, 1985, and revision received May 27, 1987.

See NAPS document No. 04526 for 13 pages of supplementary material. Order from NAPS c/o Microfiche Publications, P.O. Box 3513, Grand Central Station, New York, NY 10163. Remit in advance in U.S. funds only $7.75 for photocopies or $4.00 for microfiche. Outside the U.S. and Canada, add postage of $4.50 for the first 20 pages and $1.00 for each of 10 pages of material thereafter, $1.50 for microfiche postage.